Nonlinear Analysis: Real World Applications 17 (2014) 147–160

Contents lists available at ScienceDirect

Nonlinear Analysis: Real World Applications

journal homepage: www.elsevier.com/locate/nonrwa

Backward bifurcation in a mathematical model for HIV infection *in vivo* with anti-retroviral treatment

Michael Y. Li [a], Liancheng Wang [b,*]

[a] *Department of Mathematical and Statistical Sciences, University of Alberta, Edmonton, Alberta, T6G 2G1 Canada*

[b] *Department of Mathematical and Statistical Sciences, Kennesaw State University, 1000 Chastain Rd., #1601, Kennesaw, GA 30144, USA*

ARTICLE INFO

Article history:
Received 15 November 2012

ABSTRACT

Anti-retroviral treatments (ART) such as HAART have been used to control the replication of HIV virus in HIV-positive patients. In this paper, we study an in-host model of HIV infection with ART and carry out mathematical analysis of the global dynamics and bifurcations of the model in different parameter regimes. Among our discoveries is a parameter region for which backward bifurcation can occur. Biologically, the catastrophic behaviors associated with backward bifurcations may explain the sudden rebound of HIV viral load when ART is stopped, and possibly provide an explanation for the viral blips during ART suppression of HIV.

1. Introduction

Human immunodeficiency virus (HIV) type I is an RNA virus that preferentially targets the $CD4^+$ helper T cells. After entry into a target cell, the viral RNA is reverse transcribed into viral DNA using host genetic materials and viral reverse transcriptase. The viral DNA is transported to the cell nucleus and integrated into the host genome through the action of viral integrase and stays latent. Upon antigenic stimulation, the viral DNA can be transcribed into new viral RNA and viral proteins such as reverse transcriptase, integrase and protease. The viral protease is needed in this stage to cut the long polypeptide chain into individual enzyme components to complete the translation of viral proteins. At this stage, the target cell is called *productively infected*. The viral RNA genome and viral proteins will be assembled and enveloped to become mature virus near the cell membrane. Mature viruses bud out of the host cell and get released into the plasma to infect new target cells. Viral budding will terminate an infected $CD4^+$ T cells. In addition, HIV infection can lead to increased rate of apoptosis of a target cell, and an infected target cell can be recognized and lysed by the CD8 cytotoxic T cells. These factors combine to progressively reduce the number of $CD4^+$ T cells in the body and leave the body increasingly susceptible to opportunistic infections. Anti-retroviral drugs are designed to block the action of various HIV viral proteins and hence interrupt the viral replication cycle. Reverse transcriptase inhibitor (RTI) based drugs can block the reverse transcription of viral DNA and prevent the host cell from becoming productively infected. Protease inhibitor (PI) based drugs aim to block the action of protease and thus prevent the production of mature viruses. Due to the extremely high rate of mutation of HIV, standard ART regimens combine several drugs from both RTI and PI family to avoid emergence of drug resistance. Mathematical models have been developed to describe the HIV infection dynamics and effects of ART [1–13]. These in-host models are useful for exploring possible mechanisms and outcomes of the viral infection process [1,5,3], and for estimating key parameter values such as virion clearance rate, life span of infected cells, and average viral generation time *in vivo* [2]. Findings from in-host modeling can be used to guide development of efficient antiviral drug therapies [4].

* Corresponding author. Tel.: +1 678 797 2139; fax: +1 770 423 6629.
E-mail addresses: mli@math.ualberta.ca (M.Y. Li), lwang5@kennesaw.edu (L. Wang).

1468-1218/$ – see front matter © 2013 Elsevier Ltd. All rights reserved.
http://dx.doi.org/10.1016/j.nonrwa.2013.11.002

To model the HIV infection process, target cell ($CD4^+$ T cells) population is partitioned into uninfected T and productively-infected T^* compartment, with $T(t)$ and $T^*(t)$ representing their concentrations at time t, respectively. A compartment V of free HIV viruses is considered with concentration $V(t)$ at time t. The infection is customarily assumed to be through entry of a target cell by free viruses, though recent evidences show that HIV viruses can be transmitted through direct cell-to-cell contact [14]. A typical model for the HIV infection is described by the following system of differential equations:

$$\begin{aligned} \dot{T} &= s - \alpha T - kVT + f(T, T^*), \\ \dot{T}^* &= kVT - \beta T^* + g(T, T^*), \\ \dot{V} &= N\beta T^* - \epsilon V. \end{aligned} \tag{1}$$

In the model, target cells are assumed to be produced from precursors at a constant rate s. Turn-over rates for the uninfected target cells, productively-infected target cells, and viruses are denoted by α, β, and ϵ, respectively. It is biologically plausible to assume that infected target cells have a higher turn-over rate than uninfected cells, namely, $\beta \geq \alpha$. The incidence of infection through contact between viruses and healthy target cells is assumed to follow a simple mass-action term kVT, where constant $k > 0$ is the transmission coefficient. Infected T cells are assumed to produce on average N mature viruses during its lifetime. The model parameters are assumed to be positive.

Functions f and g describe target-cell dynamics, including cell turn-over and proliferation through mitosis. An earlier model of Nowak and May [7] assumed that T cells do not proliferate ($f = 0, g = 0$). Perelson and Nelson [5] and Leenheer and Smith [9] incorporated proliferation in uninfected target cells with a simplified logistic form $f = rT(1 - T/T_m)$ and $g = 0$, where r is the proliferation rate and T_m is the capacity of target cell population at which proliferation stops. With this simplified logistic form, system (1) is competitive, and complete mathematical analysis is carried out by Leenheer and Smith [9] using the theory for three dimensional competitive systems. Wang and Li [10] incorporated a full logistic proliferation term for uninfected target cells with $f = rT(1 - (T + T^*)/T_m)$ and $g = 0$. Wang and Ellermeyer [11] incorporated a full logistic form in both uninfected and infected cell populations with $f = g = rT(1 - (T + T^*)/T_m)$. Mathematical analysis of the global dynamics depends on the forms of f and g. With $f = g = 0$, simple threshold dynamics can be established using global Lyapunov functions as in [15]. With a simplified logistic f and $g = 0$, global dynamics of system (1) are established in [9] using the theory of monotone dynamical systems. With full logistic f and g, system (1) is no longer monotone, and global Lyapunov functions used in the literature are not effective because of the logistic terms. Global dynamics are analyzed using the Li–Muldowney approach developed by Li and Muldowney [16].

ART therapies using RTI and PI based drugs have been incorporated into HIV infection models with either no proliferation terms or a simplified logistic proliferation (e.g. [2,4,7,12,13]). In this paper, we investigate a class of HIV infection models with full logistic proliferation and incorporating RTI-based ART. The model takes the following form:

$$\begin{aligned} \dot{T} &= s - \alpha T + r_1 T\left(1 - \frac{T + T^*}{T_m}\right) - kVT, \\ \dot{T^*} &= \sigma kVT - \beta T^* + r_2 T^*\left(1 - \frac{T + T^*}{T_m}\right), \\ \dot{V} &= N\beta T^* - \epsilon V, \end{aligned} \tag{2}$$

where $0 \leq 1 - \sigma \leq 1$ is the rate of reduction in numbers of productively-infected target cells due to interruption of reverse transcription by the RTI-based drugs. Parameter $1 - \sigma$ is a measure of the efficiency of the ART; if $\sigma = 0$, HIV infection produces no productively-infected target cells, and ART is 100% effective, and if $\sigma = 1$, then ART has no effect. The effect of PI-based drugs is to reduce the number N of mature virus released from a single infected target cell. We will focus on the effects of RTI-based ART in this study. We assume that uninfected and productively-infected T cells proliferate at different rates r_1 and r_2, respectively. It is biologically plausible to expect that uninfected T cells have a greater growth rate than infected T cells, namely, $r_1 \geq r_2$. When $\sigma = 1$ and $r_1 = r_2 = r$, system (2) reduces to that studied in [11]. When $\sigma = 1$ and $r_2 = 0$, system (2) reduces to earlier models considered in [5,9,10].

The main objective of the paper is to establish that the combination of ART and proliferation among infected target cells provides a mathematically sound and biologically plausible mechanism for backward bifurcation, and that ART may bring unexpected effects such as bi-stability and hysteresis that are typically associated with backward bifurcations. It is known in the HIV/AIDS literature that, among most HIV patients, successful ART therapies can suppress HIV replication to undetectable levels. It is also known that failure or stoppage of ART can lead to prompt (within 2–3 weeks) viral rebound to significant levels after long-term suppression [17–20], even when viral reservoir is extremely low among resting $CD4^+$ T cells [19]. The hysteresis property associated with the backward bifurcation that is shown to exist in model (2) (Theorem 7) implies that prompt viral rebound is possible without the existence of viral reservoir. The bi-stability property due to the backward bifurcation may also help explain transient viral blips observed among patients under ART treatment, when the stochastic effect may shift the viral load between the basin of attractions of the stable infection-free steady state and a stable chronic infection steady state.

To establish our results, we carry out mathematical analysis on the existence and number of steady states, local stability of infection-free and chronic-infection steady states. We identify parameter regimes in which backward bifurcation occurs and derive related threshold parameters. To completely describe the global dynamics, we have also established the global

stability of the infection-free steady state when it is the only steady state, and that of the chronic steady state when it is unique. Our proof of the infection-free steady state is new and is developed to handle the logistic terms. Our proof of global stability of the unique chronic-infection steady state uses the geometric approach of Li–Muldowney. To relate our mathematical results to the biological context, we have derived the basic reproduction number R_0, as a function of σ, and interpreted our mathematical results in terms of R_0. Numerical simulations using biologically plausible parameter values are used to demonstrate our theoretical results and show their biological implications.

Backward bifurcations have been widely studied in the literature of epidemic models, and several mechanisms including imperfect immunity, leaky vaccines and behavioral responses to perceived disease risk have been identified to lead to backward bifurcations [21–31]. Backward bifurcation is shown to occur by Gomez and Li [29] in a simple in-host model of viral infection through direct cell-to-cell transmission. The mechanism for backward bifurcation is the combination of partial immune protection and target-cell proliferation. This mechanism is very similar to what we establish in the present paper for viral infections through free virus, since ART only provides partial protection from viral infection. HIV infection is recently known to occur through both virus-to-cell and cell-to-cell transmissions, results in [29] and the present paper together show that backward bifurcation may be intrinsic to the viral dynamics of HIV in the present ART environment. Our model (2) has ignored many factors that have been considered in the HIV modeling literature, such as intra-cellular delays, latently infected cells and CTL response. Nonetheless, model (2) represents a simple mathematical model for the viral dynamics of HIV with a virologically plausible mechanism for backward bifurcation and the associated bi-stability.

2. Feasible region and steady states

It can be verified that the nonnegative orthant $\mathbb{R}^3_+ = \{(T, T^*, V) : T \geq 0, T^* \geq 0, V \geq 0\}$ is positively invariant with respect to system (2) and the model is well posed. In the absence of HIV infection, the target-cell dynamics are described by

$$\dot{T} = s - \alpha T + r_1 T \left(1 - \frac{T}{T_m}\right).$$

Simple phase-line analysis shows that the target-cell concentration regulates at a positive level T_0, with

$$T_0 = \frac{T_m}{2r_1}\left[(r_1 - \alpha) + \sqrt{(r_1 - \alpha)^2 + \frac{4sr_1}{T_m}}\right]. \tag{3}$$

We assume that target cells stop growing at $T = T_m$. This requires a compatibility condition $T_m > s/\alpha$. Under this condition and (3) we have the relation $T_0 \leq T_m$.

The first two equations of system (2) lead to inequality

$$\begin{aligned}\dot{T} + \dot{T}^* &\leq s - \alpha T - \beta T^* + r_1 T\left(1 - \frac{T + T^*}{T_m}\right) + r_2 T^*\left(1 - \frac{T + T^*}{T_m}\right)\\ &\leq s - \alpha(T + T^*) + r_1(T + T^*)\left(1 - \frac{T + T^*}{T_m}\right),\end{aligned}$$

since $\alpha \leq \beta$ and $r_1 \geq r_2$. Therefore, $\limsup_{t\to\infty}(T(t) + T^*(t)) \leq T_0$ for all solutions in $\mathbb{R}^3_+$, and $T(t) + T^*(t) \leq T_0$ for $t \geq 0$ if $T(0) + T^*(0) \leq T_0$. Boundedness of $T^*(t)$ and the equation of V imply that $\limsup_{t\to\infty} V$ is bounded by a constant $M > 0$ independent of initial conditions. It can then be verified that the bounded set

$$\Gamma = \{(T, T^*, V) \in \mathbb{R}^3_+ : T + T^* \leq T_0, V \leq M\}$$

is positively invariant with respect to system (2) and is globally attracting in $\mathbb{R}^3_+$. It suffices to study the global dynamics of (2) in region Γ.

Steady states (T, T^*, V) of (2) satisfy the following system of equations.

$$s - \alpha T + r_1 T\left(1 - \frac{T + T^*}{T_m}\right) - kVT = 0, \tag{4}$$

$$\sigma kVT - \beta T^* + r_2 T^*\left(1 - \frac{T + T^*}{T_m}\right) = 0, \tag{5}$$

$$N\beta T^* - \epsilon V = 0. \tag{6}$$

An *infection-free* steady state $P_0 = (T_0, 0, 0)$ exists for all positive parameter values. A *chronic-infection* steady state $P^* = (T, T^*, V)$ satisfies $T, T^*, V > 0$. From Eq. (6), we get

$$T^* = \frac{\epsilon}{N\beta}V. \tag{7}$$

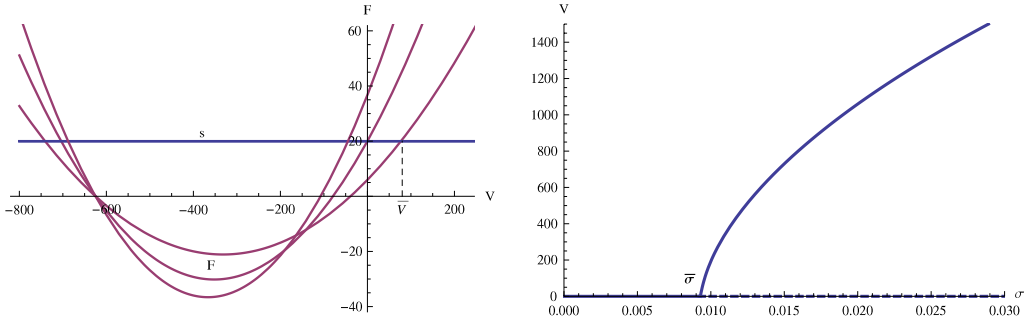

(a) Intersections of graph of F and the horizontal line at s.

(b) Bifurcation diagram showing forward bifurcation when $\beta \geq r_2$.

Fig. 1. Existence and uniqueness of infected steady state and the bifurcation diagram when $\beta \geq r_2$. We have shown in (a) three graphs of F corresponding to $\sigma < \bar{\sigma}$ $(F(0) > s)$, $\sigma = \bar{\sigma}$ $(F(0) = s)$ and $\sigma > \bar{\sigma}$ $(F(0) < s)$. The bifurcation diagram in (b) shows a forward bifurcation common to in-host models.

Substituting this relation into (5) we obtain

$$\left(\sigma k - \frac{r_2\epsilon}{N\beta T_m}\right)T = \frac{\epsilon}{N} + \frac{r_2\epsilon^2}{N^2\beta^2 T_m}V - \frac{r_2\epsilon}{N\beta}. \tag{8}$$

If $\sigma \neq \frac{r_2\epsilon}{kN\beta T_m}$, we have

$$T = \frac{\epsilon T_m(\beta - r_2)}{\sigma kN\beta T_m - r_2\epsilon} + \frac{r_2\epsilon^2}{N\beta(\sigma kN\beta T_m - r_2\epsilon)}V. \tag{9}$$

Using (7) and (9) to eliminate T and T^* from Eq. (4), we obtain a single equation for V in the form

$$s = (A + BV)(C + DV), \tag{10}$$

where

$$A = \frac{\epsilon T_m(\beta - r_2)}{\sigma kN\beta T_m - r_2\epsilon}, \qquad B = \frac{r_2\epsilon^2}{N\beta(\sigma kN\beta T_m - r_2\epsilon)},$$
$$C = (\alpha - r_1) + \frac{r_1\epsilon(\beta - r_2)}{\sigma kN\beta T_m - r_2\epsilon}, \qquad D = k\frac{\sigma(r_1\epsilon + kN\beta T_m) - r_2\epsilon}{\sigma kN\beta T_m - r_2\epsilon}.$$

Define

$$\sigma_1 = \frac{r_2\epsilon}{kN\beta T_m + r_1\epsilon} \quad \text{and} \quad \sigma_2 = \frac{r_2\epsilon}{kN\beta T_m}. \tag{11}$$

Then we have $\sigma_1 < \sigma_2$. We assume that $\sigma_2 < 1$. Let

$$F(V) = (A + BV)(C + DV), \tag{12}$$

and define

$$\bar{\sigma} = \frac{r_2\epsilon}{kN\beta T_m} + \frac{\epsilon(\beta - r_2)}{kN\beta T_0} = \frac{\epsilon}{kN\beta T_0}\left(\frac{sr_2}{r_1 T_0} + \frac{\beta r_1 - \alpha r_2}{r_1}\right). \tag{13}$$

Then $\bar{\sigma} > 0$ since $s - \alpha T_0 + r_1 T_0(1 - T_0/T_m) = 0$ and $\beta \geq \alpha, r_1 \geq r_2$.

Proposition 1. *Assume that $\beta \geq r_2$. Then*

- *if $\sigma \leq \bar{\sigma}$, system (2) has no chronic-infection steady states;*
- *if $\sigma > \bar{\sigma}$, system (2) has a unique chronic-infection steady state P^*.*

Proof. Assume that $\beta \geq r_2$. If $\sigma < \sigma_2 \leq \bar{\sigma}$, then $A \leq 0$ and $B < 0$, and $T = A + BV \leq 0$. There is no infected steady state P^* in this case. If $\sigma = \sigma_2$, then Eq. (8) implies that $V = N\beta T_m(r_2 - \beta)/r_2\epsilon \leq 0$, and P^* does not exist. If $\beta = r_2$, then $\sigma_2 = \bar{\sigma}, A = 0$, and $C = \alpha - r_1 \leq \alpha - \beta \leq 0$. In this case, equation $F(V) = s$ has a positive solution if and only if $\sigma > \sigma_2 = \bar{\sigma}$.

Suppose that $\beta > r_2$ and $\sigma > \sigma_2$. Then $\sigma_2 < \bar{\sigma}, A > 0, B > 0$, and $D > 0$. The function $F(V)$ is concave up with at least one negative root. If $C > 0$, then both roots of $F(v)$ are negative, see Fig. 1(a). The graph of $F(V)$ has exactly one intersection

with the horizontal line at s if and only if $F(0) < s$. The equality $F(0) = s$ will define the threshold value for σ. In this case, $V = 0$ and $T^* = 0$, and thus $T = T_0$. Using Eq. (8) we obtain

$$F(0) = s \iff \sigma = \bar{\sigma}$$

and using $F(0) = AC$ we get

$$F(0) < s \iff \sigma > \bar{\sigma}.$$

If $C < 0$, then the expression of C implies that $r_1 > \alpha$ and

$$\begin{aligned}\sigma &> \frac{\epsilon}{kN\beta T_0}\left[\frac{r_2 T_0}{T_m} + \frac{r_1 T_0}{(r_1-\alpha)T_m}(\beta - r_2)\right] \\ &> \frac{\epsilon}{kN\beta T_0}\left[\frac{r_2 T_0}{T_m} + \beta - r_2\right] = \bar{\sigma},\end{aligned}$$

since, from Eq. (3)

$$\frac{r_1 T_0}{(r_1-\alpha)T_m} > 1.$$

In this case, $F(V)$ has one positive root and one negative root, and its graph intersects the horizontal line at s exactly once. □

The bifurcation diagram illustrating results in Proposition 1 is shown in Fig. 1(b).

We now discuss the existence of P^* when $\beta < r_2$. Suppose that $0 \le \sigma < \sigma_1$. Then $A > 0$, $B < 0$, and $D > 0$. Without loss of generality, we assume that $C > 0$. Then F is concave down and has two zeros $-A/B > 0$ and $-C/D < 0$. Again, using $F(0) = AC$ we can show that, in this case, $F(0) < s$ if and only if $\sigma < \bar{\sigma}$. Function F has its maximum value

$$F_{\max}(\sigma) = -\frac{(AD-BC)^2}{4BD} = -\frac{[kN\beta T_m(r_2-\beta) + \epsilon(r_2\alpha - r_1\beta)]^2}{4kN\beta r_2(\sigma kN\beta T_m + \sigma r_1\epsilon - r_2\epsilon)} > 0$$

achieved at

$$V_* = -\frac{1}{2}\left(\frac{A}{B} + \frac{C}{D}\right). \tag{14}$$

We assume that $V_* > 0$. It is easy to see that $F_{\max}(\sigma)$ is increasing with σ in the interval $[0, \sigma_1)$. Solving the equation

$$F_{\max} = -\frac{[kN\beta T_m(r_2-\beta) + \epsilon(r_2\alpha - r_1\beta)]^2}{4kN\beta r_2(\sigma kN\beta T_m + \sigma r_1\epsilon - r_2\epsilon)} = s$$

for σ, we get

$$\sigma^* = \frac{r_2\epsilon}{kN\beta T_m + r_1\epsilon} - \frac{[kN\beta T_m(r_2-\beta) + \epsilon(r_2\alpha - r_1\beta)]^2}{4kN\beta r_2 s(kN\beta T_m + r_1\epsilon)}. \tag{15}$$

We assume that

$$F_{\max}(0) = \frac{[kN\beta T_m(r_2-\beta) + \epsilon(r_2\alpha - r_1\beta)]^2}{4kN\beta r_2^2\epsilon} < s. \tag{16}$$

The following relationship then holds:

$$0 < \sigma^* < \bar{\sigma} < \sigma_1 < \sigma_2. \tag{17}$$

Proposition 2. *Assume that $\beta < r_2$ and $V_* > 0$. Then*

(i) *if $0 \le \sigma < \sigma^*$, system (2) has no chronic-infection steady states;*
(ii) *if $\sigma = \sigma^*$, system (2) has a unique chronic-infection steady state P^*;*
(iii) *if $\sigma^* < \sigma < \bar{\sigma}$, system (2) has exactly two chronic-infection steady states P_* and P^*;*
(iv) *if $\sigma \ge \bar{\sigma}$, system (2) has a unique chronic-infection steady state P^*.*

Proof. If $\sigma < \sigma_1$, then F is concave down and its maximum value increases with σ. When $\sigma < \sigma^*$, the maximum F is less than s, and its graph has no intersections with the horizontal line l at s. When $\sigma = \sigma^*$, the graph of F is tangent to the horizontal line l, resulting in a unique chronic-infection steady state P^*. As σ increases through σ^* the graph of F will intersect l at two points, resulting in two chronic-infection steady states $P_* = (T_1, T_1^*, V_1)$ and $P^* = (T_2, T_2^*, V_2)$ with $V_1 < V_2$ and $T_1 > T_2$. When σ further increases beyond $\bar{\sigma}$, we have $F(0) > s$, and the graph of F has only one intersection with l in the first quadrant. See Fig. 2 for an illustration. □

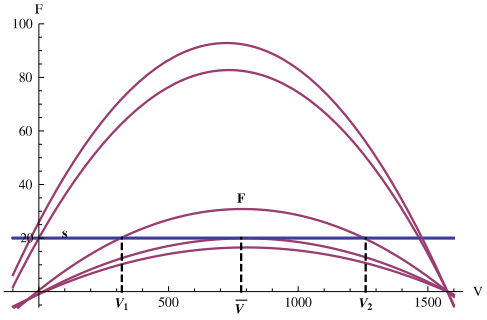

(a) Intersection of graphs of F and the horizontal line at s when $\beta < r_2$.

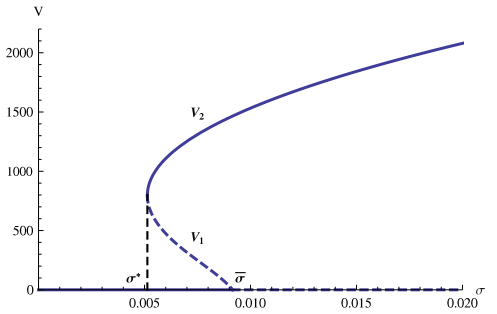

(b) Bifurcation diagram showing a backward bifurcation when $\beta < r_2$.

Fig. 2. Existence and number of chronic-infection steady states and the bifurcation diagram when $\beta < r_2$. We have shown in (a) five graphs of F corresponding to $\sigma < \sigma^*$, $\sigma = \sigma^*$, $\sigma^* < \sigma < \bar{\sigma}$, $\sigma = \bar{\sigma}$, and $\sigma > \bar{\sigma}$. The bifurcation diagram in (b) shows a backward bifurcation at $\sigma = \bar{\sigma}$.

3. Local stability analysis

3.1. Stability of the infection-free steady state P_0

The Jacobian matrix of system (2) at $P_0 = (T_0,\ 0,\ 0)$ is

$$J(P_0) = \begin{bmatrix} -\alpha + r_1 - \dfrac{2r_1T_0}{T_m} & -\dfrac{r_1T_0}{T_m} & -kT_0 \\ 0 & -\beta + r_2 - \dfrac{r_2T_0}{T_m} & \sigma kT_0 \\ 0 & N\beta & -\epsilon \end{bmatrix}.$$

One eigenvalue of $J(P_0)$ is

$$-\alpha + r_1\left(1 - \frac{2T_0}{T_m}\right) = -\frac{s}{T_0} - \frac{r_1T_0}{T_m} < 0,$$

by Eq. (4). The remaining two eigenvalues are solutions of the quadratic equation

$$\lambda^2 + \left(\beta - r_2 + \frac{r_2T_0}{T_m} + \epsilon\right)\lambda + \beta\epsilon - r_2\epsilon\left(1 - \frac{T_0}{T_m}\right) - \sigma kN\beta T_0 = 0,$$

and they have negative real part if and only if $\beta\epsilon - r_2\epsilon\left(1 - \frac{T_0}{T_m}\right) - \sigma kN\beta T_0 > 0$, which is equivalent to $\sigma < \bar{\sigma}$. We have the following result.

Theorem 3. *If $\sigma < \bar{\sigma}$, then P_0 is locally asymptotically stable. If $\sigma > \bar{\sigma}$, then P_0 is unstable.*

3.2. Stability of chronic-infection steady states P^* and P_*

The Jacobian matrix at $P = (T, T^*, V)$ ($P = P^*$ or $P = P_*$) is

$$J(P) = \begin{bmatrix} -\alpha + r_1\left(1 - \dfrac{T+T^*}{T_m}\right) - \dfrac{r_1T}{T_m} - kV & -\dfrac{r_1T}{T_m} & -kT \\ \sigma kV - \dfrac{r_2T^*}{T_m} & -\beta + r_2\left(1 - \dfrac{T+T^*}{T_m}\right) - \dfrac{r_2T^*}{T_m} & \sigma kT \\ 0 & N\beta & -\epsilon \end{bmatrix},$$

where $T, T^*, V > 0$. From the equilibrium equations we obtain

$$\alpha - r_1\left(1 - \frac{T+T^*}{T_m}\right) + kV = \frac{s}{T}, \qquad \beta - r_2\left(1 - \frac{T+T^*}{T_m}\right) = \frac{\sigma kVT}{T^*}, \qquad \epsilon = \frac{N\beta T^*}{V}.$$

The characteristic polynomial of $J(P)$ can be written as

$$P(\lambda) = \lambda^3 + a_1\lambda^2 + a_2\lambda + a_3,$$

Table 1
Existence, number and stability of steady states of model (2) where LAS means locally asymptotically stable, US means unstable and GAS means globally asymptotically stable in the feasible region.

Parameter regions		Equilibria	Local stability	Global stability
$\beta \geq r_2$	$\sigma \leq \bar{\sigma}$	P_0	P_0 LAS	P_0 GAS
	$\sigma > \bar{\sigma}$	P_0, P^*	P_0 US, P^* LAS	P^* GAS[b]
$\beta < r_2$ and $V^* > 0$	$0 \leq \sigma < \sigma^*$	P_0	P_0 LAS	
	$\sigma^* < \sigma < \bar{\sigma}$	P_0, P_*, P^*	P_0, P^* LAS[a], P_* US	
	$\sigma > \bar{\sigma}$	P_0, P^*	P_0 US, P^* LAS[a]	

[a] LAS under condition (19).
[b] GAS under condition (26).

with

$$\begin{aligned} a_1 &= \frac{s}{T} + \frac{r_1 T}{T_m} + \frac{\sigma k V T}{T^*} + \frac{r_2 T^*}{T_m} + \epsilon > 0, \\ a_2 &= \frac{s}{T}\left(\frac{\sigma k V T}{T^*} + \frac{r_2 T^*}{T_m} + \epsilon\right) + \frac{\epsilon}{T_m}\left(r_1 T + r_2 T^*\right) + \frac{\sigma r_1 k T V}{T_m T^*}(T + T^*) > 0, \\ a_3 &= \frac{\sigma k^2 \epsilon T V^2}{T^*} + \frac{s r_2 \epsilon T^*}{T T_m} + (\sigma r_1 - r_2)\frac{k \epsilon T V}{T_m} = \frac{1}{T_m}(\sigma k N \beta T_m - r_2 \epsilon) V F'(V), \end{aligned} \tag{18}$$

where $F(V)$ is defined in (12). Assume that

$$a_1 a_2 - a_3 > 0. \tag{19}$$

Then the Routh–Hurwitz stability conditions imply that all eigenvalues of $J(P)$ have negative real parts if and only if $a_3 > 0$ at P. We arrive at the following result.

Theorem 4. *Assume that $a_1 a_2 > a_3$. Then, when it exists, a chronic-infection steady state $P = (T, T^*, V)$ is locally asymptotically stable if and only if $(\sigma - \sigma_2) F'(V) > 0$. In particular,*

(a) *if $\beta \geq r_2$, then P^* is unique and locally asymptotically stable when it exists; and*
(b) *if $\beta < r_2$ and $V_* > 0$, then P_* is unstable and P^* is stable when they exist.*

We have summarized our results on the existence and local stability of steady states in Table 1. Global stability results will be established in the next section.

Using (19), we can derive sufficient conditions for our assumption $ab > c$. One of them is

$$\alpha - r_1 + r_1 \frac{T + T^*}{T_m} > 0.$$

We can see that if r_1 is sufficiently small P^* is locally asymptotically stable. We also note that relation $ab > c$ may not always hold and P^* may not be stable in certain parameter ranges. In Fig. 3, we show a case when P^* is unstable and a stable periodic solution exists for system (2). The parameter values used for the simulation are: $s = 0.1$, $k = 0.0027$, $\epsilon = 2.4$, $\alpha = 0.2$, $\beta = 1$, $r_1 = 0.55$, $r_2 = 0.5$, $T_m = 1500$, $N = 10$ and $\sigma = 0.7$. Periodic solutions have been discovered in other viral dynamics models (e.g. [10–12]). Though they are shown to exist mathematically, sustained oscillations in viral load and CD4 count have not been observed among HIV patients. A likely reason is that the parameter values for which periodic solutions exist may not be biologically relevant.

4. Global stability analysis when $\beta > r_2$

4.1. Global stability of P_0

Theorem 5. *Assume that $\beta > r_2$. Then the infection-free steady state P_0 is globally asymptotically stable in the feasible region Γ if $\sigma < \bar{\sigma}$.*

Proof. Relation

$$\sigma < \bar{\sigma} = \frac{r_2 \epsilon}{k N \beta T_m} + \frac{\epsilon(\beta - r_2)}{k N \beta T_0}$$

is equivalent to

$$-(\beta - r_2) + \left(\frac{\sigma N \beta k}{\epsilon} T_m - r_2\right)\frac{T_0}{T_m} < 0. \tag{20}$$

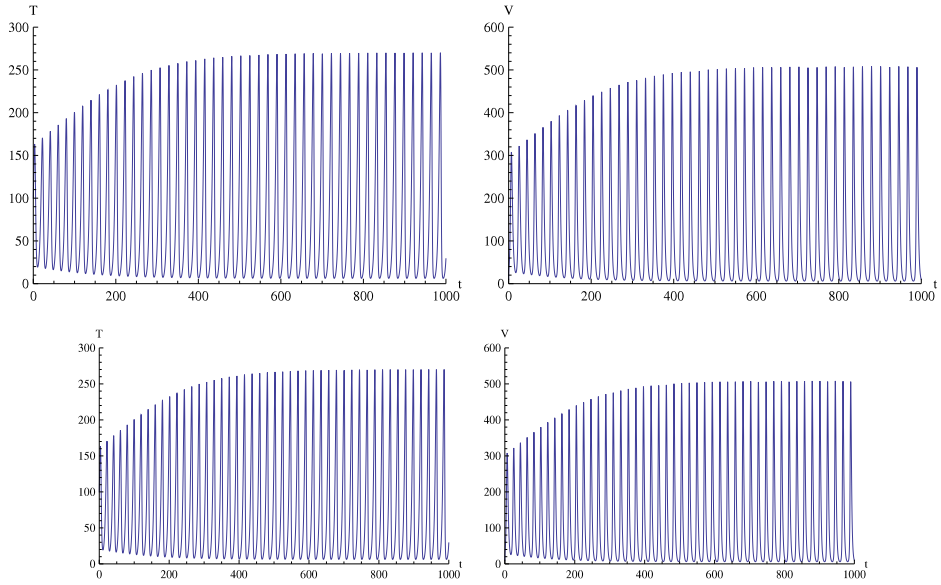

Fig. 3. Numerical simulations showing the existence of a stable periodic solution of model (2).

Since P_0 is shown to be locally asymptotically stable in Theorem 4, it suffices to show that P_0 globally attracts in the feasible region Γ. A solution $(T(t), T^*(t), V(t))$ to model (2) in Γ satisfies

$$\begin{bmatrix} \dot{T}^* \\ c\dot{V} \end{bmatrix} = A(t) \begin{bmatrix} T^* \\ cV \end{bmatrix}, \tag{21}$$

where $c > 0$ is a constant to be specified, with

$$A(t) = \begin{bmatrix} -\beta + r_2\left[1 - \dfrac{T(t) + T^*(t)}{T_m}\right] & \dfrac{\sigma k T(t)}{c} \\ cN\beta & -\epsilon \end{bmatrix}.$$

Let $|\cdot|$ denote the l_∞ norm in $\mathbb{R}^2$ and μ_∞ the Lozinskiĭ measure with respect to $|\cdot|$, see Appendix. From the discussion in the Appendix we obtain the following relations:

$$\frac{d^+}{dt} \max\{T^*(t), cV(t)\} \le \mu_\infty(A(t))\ \max\{T^*(t), cV(t)\},$$

where $\frac{d^+}{dt}$ denotes the right derivative, and

$$\mu_\infty(A(t)) = \max\left\{-\beta + r_2[1 - (T + T^*)/T_m] + \frac{\sigma kT}{c},\ cN\beta - \epsilon\right\}. \tag{22}$$

We want to show that $\mu_\infty(A(t)) \le -\eta < 0$ for all $t \ge 0$, which then implies that $\max\{T^*(t), dV(t)\} \to 0$ as $t \to \infty$, and hence that P_0 globally attracts.

Set $c = \frac{\beta N + \delta}{\epsilon}$. Using relations (20) and $\beta > r_2$, we can choose $\delta, \eta > 0$ sufficiently small that

$$cN\beta - \epsilon < -\eta, \qquad -\beta + r_2 + \frac{\sigma kT_0}{\epsilon}\delta < -\eta, \tag{23}$$

and

$$-\beta + r_2 + \left(\frac{\sigma N\beta k}{\epsilon}T_m - r_2\right)\frac{T_0}{T_m} + \frac{\sigma kT_0}{\epsilon}\delta < -\eta. \tag{24}$$

Therefore,

$$-\beta + r_2\left[1 - \frac{T + T^*}{T_m}\right] + \frac{\sigma kT}{c} \le -\beta + r_2 + \left[\frac{\sigma N\beta k}{\epsilon}T_m - r_2\right]\frac{T}{T_m} + \frac{\delta\sigma kT_0}{\epsilon}. \tag{25}$$

If $\sigma < \sigma_2 = \frac{r_2\epsilon}{kN\beta T_m}$, then $\frac{\sigma N\beta kT_m}{\epsilon} < r_2$, and it follows from (22), (23) and (25) that

$$\mu_\infty(A(t)) < -\eta, \quad \text{for all } t \geq 0.$$

If $\sigma \geq \sigma_2 = \frac{r_2\epsilon}{kN\beta T_m}$, then $\frac{\sigma N\beta kT_m}{\epsilon} \geq r_2$, and thus

$$-\beta + r_2 + \left[\frac{\sigma N\beta k}{\epsilon}T_m - r_2\right]\frac{T}{T_m} \leq -\beta + r_2 + \left[\frac{\sigma N\beta k}{\epsilon}T_m - r_2\right]\frac{T_0}{T_m}.$$

This relation, together with (22)–(24), implies $\mu_\infty(A(t)) < -\eta$ for all $t \geq 0$, completing the proof. □

4.2. Global stability of the unique chronic-infection equilibrium P^*

We will apply the Li–Muldowney global-stability criterion as summarized in the Appendix to show the global stability of P^*. To verify the basic assumptions of Theorem 8, we note that the interior of the feasible region $\mathring{\Gamma}$ is simply connected, and there exists a unique chronic-infection steady state P^* in $\mathring{\Gamma}$ when $\sigma > \bar{\sigma}$. Instability of the boundary steady state P_0 when $\sigma > \bar{\sigma}$ implies that system (2) is uniformly persistent [32,33]. Uniform persistence, together with ultimate boundedness of solutions, implies the existence of a compact absorbing set $K \subset \mathring{\Gamma}$ [34].

Theorem 6. *Assume that $\beta > r_2$ and $\alpha > r_1$. Then, when $\sigma > \bar{\sigma}$, the unique chronic-infection steady state P^* is globally asymptotically stable in $\mathring{\Gamma}$, provided the following condition holds:*

$$\nu = \max\left\{-\alpha + r_1 + \frac{r_2T_0}{\sigma T_m},\ -\beta + r_2 + \frac{\sigma r_1T_0}{T_m}\right\} < 0. \tag{26}$$

Proof. To apply Theorem 8, we need to show the existence of a function Q and a Lozinskiĭ measure μ such that $\bar{q}_2$ defined in (34) in the Appendix satisfies $\bar{q}_2 < 0$.

The Jacobian matrix J associated with the general solution $(T(t), T^*(t), V(t))$ to (2) is

$$J = \begin{bmatrix} -p & -\frac{r_1T}{T_m} & -kT \\ \sigma kV - \frac{r_2T^*}{T_m} & -q & \sigma kT \\ 0 & N\beta & -\epsilon \end{bmatrix},$$

where $p = \alpha - r_1\left(1 - \frac{T+T^*}{T_m}\right) + \frac{r_1T}{T_m} + kV$ and $q = \beta - r_2\left(1 - \frac{T+T^*}{T_m}\right) + \frac{r_2T^*}{T_m}$, and its second additive compound matrix $J^{[2]}$ is, by (33) in the Appendix,

$$J^{[2]} = \begin{bmatrix} -p-q & \sigma kT & kT \\ N\beta & -p-\epsilon & -\frac{r_1T}{T_m} \\ 0 & \sigma kV - \frac{r_2T^*}{T_m} & -q-\epsilon \end{bmatrix}.$$

Set the function $Q(x) = Q(T, T^*, V) = \mathrm{diag}\{1, T^*/V, T^*/(\sigma V)\}$. Then $Q_fQ^{-1} = \mathrm{diag}\{0,\ \dot{T}^*/T^* - \dot{V}/V, \dot{T}^*/T^* - \dot{V}/V\}$, and

$$\begin{aligned} X &= Q_fQ^{-1} + QJ^{[2]}Q^{-1} \\ &= \begin{bmatrix} -p-q & \frac{\sigma kTV}{T^*} & \frac{\sigma kTV}{T^*} \\ \frac{N\beta T^*}{V} & \frac{\dot{T}^*}{T^*} - \frac{\dot{V}}{V} - p - \epsilon & -\frac{\sigma r_1T}{T_m} \\ 0 & kV - \frac{r_2T^*}{\sigma T_m} & \frac{\dot{T}^*}{T^*} - \frac{\dot{V}}{V} - q - \epsilon \end{bmatrix} = \begin{bmatrix} X_{11} & X_{12} \\ X_{21} & X_{22} \end{bmatrix}, \end{aligned}$$

where $X_{11} = -p - q$, $X_{12} = [\sigma kTV/T^*, \sigma kTV/\sigma T^*]$, $X_{21} = [N\beta T^*/V, 0]^T$, and

$$X_{22} = \begin{bmatrix} \frac{\dot{T}^*}{T^*} - \frac{\dot{V}}{V} - p - \epsilon & -\frac{\sigma r_1T}{T_m} \\ kV - \frac{r_2T^*}{\sigma T_m} & \frac{\dot{T}^*}{T^*} - \frac{\dot{V}}{V} - q - \epsilon \end{bmatrix}.$$

Consider the norm $|(u, v, w)| = \max\{|u|, |v| + |w|\}$ in $\mathbb{R}^3$. Let μ be the Lozinskiĭ measure with respect to this norm. Then we have the following estimate, see [32,35],

$$\mu(X) \le \max\{g_1, g_2\} \tag{27}$$

with

$$g_1 = \mu_1(X_{11}) + |X_{12}|, \quad \text{and} \quad g_2 = |X_{21}| + \mu_1(X_{22}),$$

and $|X_{12}|$, $|X_{21}|$ are the matrix norm induced from the l_1 vector norm of $\mathbb{R}^2$, and μ_1 is the Lozinskiĭ measure with respect to the l_1 norm. More specifically, $\mu_1(X_{11}) = -p - q$, $|X_{12}| = kTV/T^*$, $|X_{21}| = N\beta T^*/V$, and $\mu_1(X_{22})$ can be evaluated by the following [36],

$$\begin{aligned}
\mu_1(X_{22}) &= \max\left\{\frac{\dot T^*}{T^*} - \frac{\dot V}{V} - p - \epsilon + \left|kV - \frac{r_2T^*}{\sigma T_m}\right|,\ \frac{\dot T^*}{T^*} - \frac{\dot V}{V} - q - \epsilon + \frac{\sigma r_1 T}{T_m}\right\}\\
&= \frac{\dot T^*}{T^*} - \frac{\dot V}{V} - \epsilon + \max\left\{-\alpha + r_1 - \frac{r_1(T+T^*)}{T_m} - \frac{r_1T}{T_m} - kV + kV + \frac{r_2T^*}{\sigma T_m},\right.\\
&\quad \left. -\beta + r_2 - \frac{r_2(T+T^*)}{T_m} - \frac{r_2T^*}{T_m} + \frac{\sigma r_1 T}{T_m}\right\}\\
&\le \frac{\dot T^*}{T^*} - \frac{\dot V}{V} - \epsilon + \max\left\{-\alpha + r_1 + \frac{r_2T_0}{\sigma T_m},\ -\beta + r_2 + \frac{\sigma r_1 T_0}{T_m}\right\}\\
&\le \frac{\dot T^*}{T^*} - \frac{\dot V}{V} - \epsilon + \nu.
\end{aligned}$$

Using the fact that $\dot T^*/T^* = \sigma kVT/T^* - \beta + r_2(1 - (T + T^*)/T_{\max})$ and $\dot V/V = N\beta T^*/V - \epsilon$, we obtain

$$\begin{aligned}
g_1 &= -p - q + \frac{\sigma kTV}{T^*} \le \frac{\dot T^*}{T^*} - \alpha + r_1 \le \frac{\dot T^*}{T^*} + \nu,\\
g_2 &\le \frac{N\beta T^*}{V} + \frac{\dot T^*}{T^*} - \frac{\dot V}{V} - \epsilon + \nu = \frac{\dot T^*}{T^*} + \nu.
\end{aligned} \tag{28}$$

Therefore $\mu(X) \le \frac{\dot T^*}{T^*} + \nu$. Let $(T(t), T^*(t), V(t))$ be any solution initiating in K and let $\bar t$ be the uniform time such that $(T(t), T^*(t), V(t)) \in K$ for all $t \ge \bar t$. Then for $t > \bar t$ we have

$$\frac{1}{t}\int_0^t \mu(X)ds \le \frac{1}{t}\int_0^{\bar t} \mu(X)ds + \frac{1}{t}\ln\frac{T^*(t)}{T^*(\bar t)} + \frac{t - \bar t}{t}\nu.$$

The boundedness of T^* then implies that $\bar q_2 \le \nu < 0$, completing the proof. □

5. The basic reproduction number and backward bifurcation

In this section, using the method of next generation matrix as in [26], we derive the basic reproduction number $R_0(\sigma)$ of model (2), as a function of parameter σ, and study the impact of ART treatment on $R_0(\sigma)$.

Using the notations of [26], we can calculate

$$F = \begin{bmatrix} r_2\left(1 - \frac{T_0}{T_m}\right) & \sigma kT_0\\ 0 & 0\end{bmatrix} \quad \text{and} \quad V = \begin{bmatrix} -\beta & 0\\ N\beta & -\epsilon\end{bmatrix},$$

and the next generation matrix is

$$FV^{-1} = \frac{1}{\beta\epsilon}\begin{bmatrix} -\epsilon r_2\left(1 - \frac{T_0}{T_m}\right) - \sigma kN\beta T_0 & -\beta\sigma kT_0\\ 0 & 0\end{bmatrix}.$$

As the spectral radius of FV^{-1}, the basic reproduction number is given by

$$R_0(\sigma) = \frac{\sigma kN}{\epsilon}T_0 + \frac{r_2}{\beta}\left(1 - \frac{T_0}{T_m}\right). \tag{29}$$

Biologically, the basic reproduction number represents the average secondary productive infections caused by one productively infected target cell in an entirely susceptible target cell population (T_0). As we can see in (29), secondary infections comes from both horizontal virus-to-cell transmission, as described by the first term, and vertical transmission through mitosis of infected target cells, as given in the second term.

Parameters σ and N only appear in the first term, implying that both RTI-based and PI-based ART therapies only directly reduce secondary infections from horizontal transmission; they have no effects on secondary infections from vertical transmission through mitosis of infected target cells. Using (13) and (29) we can derive the following relation

$$R_0(\sigma) = 1 \iff \sigma = \bar{\sigma} \quad \text{and} \quad R_0(\sigma) < 1 \iff \sigma < \bar{\sigma}.$$

Reinterpreting results in Section 3 in terms of $R_0(\sigma)$, we have the following result.

Theorem 7. (a) *The infection-free steady state P_0 is asymptotically stable if $R_0(\sigma) < 1$, and unstable if $R_0(\sigma) > 1$.*

(b) *Assume that $a_1 a_2 > a_3$. Then*

- *the unique infected steady state P^* exists and is asymptotically stable if $R_0(\sigma) > 1$;*
- *if $\beta < r_2$ and $V_* > 0$, then two chronic-infection steady states $P_* = (T_1, T_1^*, V_1)$ and $P^* = (T_2, T_2^*, V_2)$ with $V_1 < V_2$ and $T_1 > T_2$ exist when $R_0(\sigma^*) < R_0(\sigma) < 1$. Steady state P_* is unstable and P^* is asymptotically stable.*

In the parameter regime where $\beta < r_2$ and $V_* > 0$, if σ is in the range $\sigma^* < \sigma < \bar{\sigma}$, we have $R_0(\sigma) < 1$ and two sub-threshold chronic-infection steady states P^* and P_* exist, together with the infection-free equilibrium P_0. This is the situation known as backward bifurcation, see Fig. 2. Mathematically, this creates co-existence of two attractors P_0 and P^* with their own basins of attraction. In Fig. 4, we have shown numerically computed connecting orbits from the unstable steady state P_* to the stable ones P_0 and P^*, as well as depiction of basins of attraction of P_0 and P^*, in the 3-dimensional phase space. In Fig. 5, we show numerical solutions of model (2) in this parameter regime. We see that solutions may converge to P_0 or P^* depending on their initial conditions. The parameter values used for these simulations are $s = 20$, $k = 0.00018$, $\epsilon = 0.02$, $\alpha = 0.02$, $\beta = 0.021$, $r_1 = 0.03$, $r_2 = 0.024$, $T_m = 1200$ and $N = 10$, with $\sigma^* = 0.00513438$, $\bar{\sigma} = 0.00916025$.

Biologically, bi-stability may lead to unexpected adverse consequences for ART. We also believe that the backward bifurcation and the accompanying hysteresis behaviors that are intrinsic to viral dynamics under ART can provide an explanation for several well observed clinical phenomena among HIV patients.

Dependence of outcome on initial conditions. Mathematically, the bi-stability represented by the co-existence of a stable infection-free steady state P_0 and a stable chronic-infection steady state P^* implies that the feasible region Γ is partitioned into two basins of attraction. Biologically, in the basin of attraction of P_0, ART will achieve suppression of HIV virus, whereas in the basin of attraction of P^*, the virus will persist and ART is not effective. The outcome of ART critically depends on which basin of attraction the viral load and CD4 count fall into. Using numerical simulations, we demonstrate the bi-stability of P_0 and P^* in this parameter regime in Figs. 4 and 5. Our results imply that it is essential to continue monitoring a patient's viral load and CD4 count during the course of ART treatment, to ensure they remain in the basin of attraction of P_0.

Sudden jump of viral load. As it is shown in the bifurcation diagram in Fig. 2(b), when σ increases beyond $\bar{\sigma}$, the viral load V will jump from the low V_1 branch to the high V_2 branch. Biologically, this explains the sudden jump in viral load among patients with viral suppression under ART when ART is stopped or has failed. A common explanation for the sudden viral rebound is the existence of a viral reservoir in resting $CD4^+$ T cells, in which virus can hide from the drug or the immune surveillance. It is also known, however, that sudden viral rebound from total suppression is possible even viral reservoir is extremely low among resting $CD4^+$ T cells [19]. Our results show that the hysteresis property associated with backward bifurcation makes it theoretically possible for viral load to experience sudden rebound from total suppression (with stoppage of ART) without a viable viral reservoir.

Timing of ART treatment. We can also observe from the bifurcation diagram in Fig. 2(b) that, when σ decreases to $\bar{\sigma}$, or equivalently, when R_0 decreases to 1, the viral load V will decrease along the stable V_2 branch while remaining very high. Biologically, this means that if ART is initiated when the viral load is high, it is much more difficult to achieve viral suppression within the parameter range of backward bifurcation. Our results imply that it is important to test patient's viral load in addition to CD4 count before initiation of ART. This agrees with cohort studies of HIV/AIDS patients undergoing ART treatments [37], and supports the early initiation of ART among asymptomatic HIV positive patients [38].

Viral blips. It has been clinically observed among patients under full viral suppression to experience transient jumps in viral load, a phenomenon called "viral blips" [39]. Several modeling studies have attempted to explain the mechanisms responsible for the viral blips [40,41]. The bi-stability phenomenon accompanying backward bifurcation that is shown to exist in our basic viral dynamics model with ART (Theorem 7) may explain why viral blips occur. It is plausible that stochastic fluctuations of viral load or of $CD4^+$ population due to opportunistic infections may switch the trajectory back and forth between the basin of attraction of P_0 (suppression) and that of P^* (detectable viral load). This will be further investigated in a subsequent study.

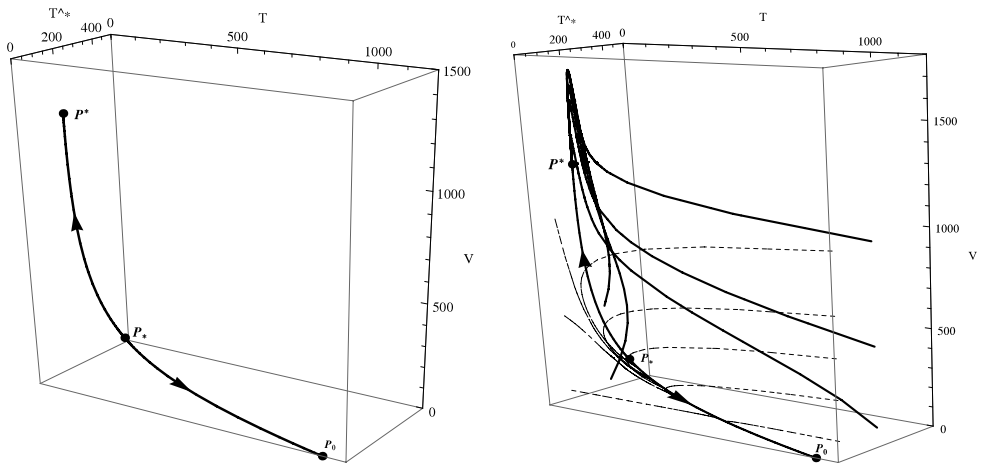

(a) Connecting orbits from P_* to P_0 and P^*. (b) Basins of attraction of P_0 and P^*.

Fig. 4. Bi-stability of sub-threshold steady states P_0 and P^* when $\beta < r_2$. Numerically computed connecting orbits from the unstable steady state P_* to the stable steady states P_0 and P^* are shown in (a). Trajectories are shown to converge to either P_0 or P^* depending on their initial positions.

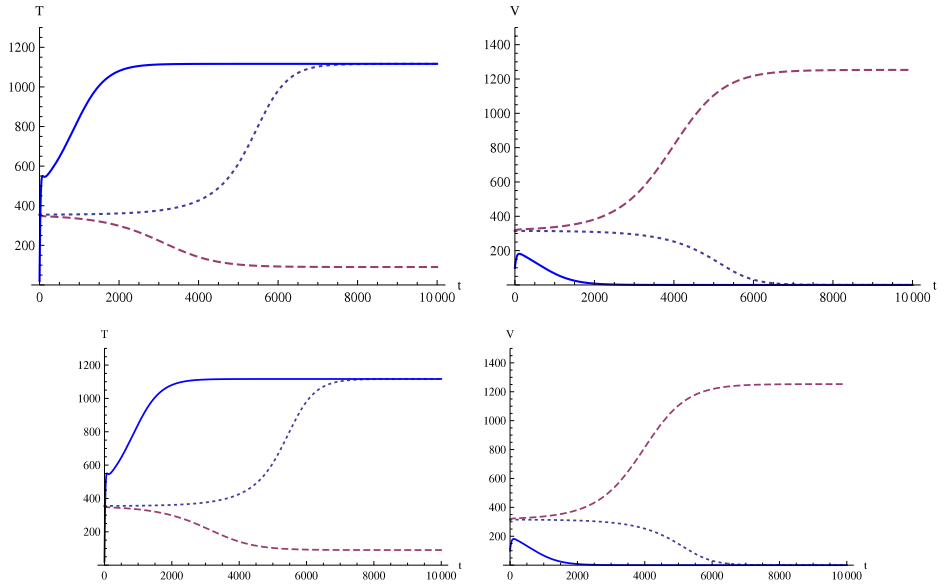

Fig. 5. Numerical solutions are shown to converge either to the infection-free steady state P_0 or to the chronic-infection steady state P^* depending on their initial conditions.

6. Summary

In this paper, we have studied a mathematical model that describes the viral dynamics of HIV with ART treatment. Our model generalizes earlier HIV models in the literature (e.g. [5,9,10]) in that it uses a full logistic term to describe the target-cell dynamics. We have analyzed the system in two different scenarios: (1) when $\beta \geq r_2$, i.e. when the death rate β of the infected target cells is greater than its proliferation rate r_2, we have shown that the model exhibits standard threshold dynamics: if the basic reproduction number $R_0 < 1$ the infection-free steady state is globally asymptotically stable and the virus is cleared; and if $R_0 > 1$ a unique infected steady state P^* is globally asymptotically stable in the interior of the feasible region, and the virus persists in the target cell population. (2) When $\beta < r_2$, we show that the viral dynamics are very different. We identify an open region of biologically relevant parameter values in which backward bifurcation occurs. We have discussed some potential adverse biological effects associated with the backward bifurcation and their implications to ART treatment. Together with the result in [29], our study shows that the combination of proliferation among HIV infected cells and partial protection against HIV infection from the ART drugs is a cause for backward bifurcation and hysteresis behaviors.

For in-host models or epidemic models with logistic terms, the global stability of the infection-free or disease-free equilibrium P_0 is of considerable challenge due to nonlinearity in the logistic terms. Our proof of the global stability of P_0 for model (2) is new and may be applicable to other models of this type.

Acknowledgments

This research is supported by a Kennesaw state University (KSU) Tenured Faculty Sabbatical Program. LW would also like to thank CSM of KSU and the University of Alberta for sponsoring and hosting his visit. Research of ML is supported in part by grants from Natural Science and Engineering Research Council (NSERC) and Canada Foundation for Innovation (CFI). Both authors would like to thank the two anonymous referees whose comments have improved the presentation of the paper.

Appendix

A.1. Lozinskiĭ measures

We summarize the definition of the Lozinskiĭ measure of matrices and its applications to differential equations. For detailed discussions we refer the reader to [36].

Let $|\cdot|$ denote a vector norm in $\mathbb{R}^n$ and also denote the induced matrix norm in $\mathbb{R}^{n\times n}$, the space of all $n\times n$ matrices. For matrix A in $\mathbb{R}^{n\times n}$, the *Lozinskiĭ measure* or the *logarithmic norm* of A with respect to $|\cdot|$ is defined as (see [36, p. 41])

$$\mu(A)=\lim_{h\to 0^+}\frac{|I+hA|-1}{h}. \tag{30}$$

Let $y(t)$ be a solution to the system of linear differential equations

$$y'(t)=A(t)y(t),$$

where $A(t)$ is an $m\times m$ matrix-valued continuous function. Then the following relation holds for the norm $|y(t)|$ and the corresponding Lozinskiĭ measure:

$$|y(t)|\le |y(t_0)|e^{\int_{t_0}^{t}\mu(A(t))\,dt},\quad \text{for } t\ge t_0. \tag{31}$$

A.2. Li–Muldowney global-stability criterion

We summarize a global-stability criterion of Li and Muldowney [16], which is used in our proof in Section 4.

Let D be an open set in $\mathbb{R}^n$, and $f: x\in D\mapsto f(x)\in\mathbb{R}^n$ be a C^1 function. Consider the differential equation

$$x'=f(x). \tag{32}$$

Denote by $x(t,x_0)$ the solution to (32) such that $x(0,x_0)=x_0$. A set K is said to be absorbing in D for system (32) if $x(t,K_1)\subset K$ for each compact set $K_1\subset D$ and sufficiently large t. Assume that the following assumptions hold:

(H_1) System (32) has a unique equilibrium point $\bar{x}$ in D.
(H_2) System (32) has a compact absorbing set $K\subset D$.

Let B be an $n\times n$ matrix in $\mathbb{R}^{n\times n}$. The second additive compound matrix of B, denoted by $B^{[2]}$, is an $\binom{n}{2}\times\binom{n}{2}$ matrix. For instance, if $B=(b_{ij})$ is a 3×3 matrix, then

$$B^{[2]}=\begin{bmatrix} b_{11}+b_{22} & b_{23} & -b_{13}\\ b_{32} & b_{11}+b_{33} & b_{12}\\ -b_{31} & b_{21} & b_{22}+b_{33}\end{bmatrix}. \tag{33}$$

For detailed discussions of compound matrices and their applications in differential equations, we refer the readers to [42,43].

Let $Q: D\longmapsto Q(x)$ be an $\binom{n}{2}\times\binom{n}{2}$ matrix-valued function that is C^1 on D, together with its inverse $Q^{-1}(x)$, and let μ be a Lozinskiĭ measure on $\mathbb{R}^{N\times N}$, where $N=\binom{n}{2}$. Define a quantity $\bar{q}_2$ as

$$\bar{q}_2=\limsup_{t\to\infty}\sup_{x_0\in K}\frac{1}{t}\int_0^t \mu(X(x(s,x_0)))ds, \tag{34}$$

where

$$X=Q_fQ^{-1}+QJ^{[2]}Q^{-1},$$

matrix Q_f is obtained by replacing each entry q_{ij} of Q by its derivative in the direction of f, $(q_{ij})_f$, and $J^{[2]}$ is the second additive compound matrix of the Jacobian matrix J of system (32). The following result is proved by Li and Muldowney in [16].

Theorem 8 (*Li and Muldowney*)**.** *For system (32), assume that D is simply connected and that assumptions (H_1) and (H_2) hold. Then the unique equilibrium $\bar{x}$ is globally asymptotically stable in D if there exist a function Q and a Lozinskiĭ measure μ such that $\bar{q}_2<0$.*

References

[1] A.S. Perelson, D.E. Kirschner, R.D. Boer, Dynamics of HIV infection of CD^{4+} T cells, Math. Biosci. 114 (1993) 81–125.
[2] A.S. Perelson, A.U. Neumann, M. Markowitz, J.M. Leonard, D.D. Ho, HIV-1 dynamics in vivo: virion clearance rate, infected cell life-span, and viral generation time, Science 271 (1996) 1582–1586.
[3] D. Kirschner, Using mathematics to understand HIV immune dynamics, Notices Amer. Math. Soc. 43 (1996) 191–202.
[4] S. Bonhoeffer, R.M. May, G.M. Shaw, M.A. Nowak, Virus dynamics and drug therapy, Proc. Natl. Acad. Sci. USA 94 (1997) 6971–6976.
[5] A.S. Perelson, P.W. Nelson, Mathematical analysis of HIV-I dynamics in vivo, SIAM Rev. 41 (1999) 3–44.
[6] R.V. Culshaw, S. Ruan, A delay-differential equation model of HIV infection of CD^{4+} T-cells, Math. Biosci. 165 (2000) 27–39.
[7] M.A. Nowak, R.M. May, Virus Dynamics, Oxford University Press, New York, 2000.
[8] P.W. Nelson, A.S. Perelson, Mathematical analysis of delay differential equation models of HIV-1 infection, Math. Biosci. 179 (2002) 73–94.
[9] P.D. Leenheer, H.L. Smith, Virus dynamics: a global analysis, SIAM J. Appl. Math. 63 (2003) 1313–1327.
[10] L. Wang, M.Y. Li, Mathematical analysis of the global dynamics of a model for HIV infection of CD^{4+} T cells, Math. Biosci. 200 (2006) 44–57.
[11] L. Wang, S. Ellermeyer, HIV infection and CD^{4+} T cell dynamics, Discrete Contin. Dyn. Syst. Ser. B 6 (2006) 1417–1430.
[12] L. Wang, Global dynamical analysis of HIV models with treatments, Internat. J. Bifur 22 (2012) http://dx.doi.org/10.1142/S0218127412502276.
[13] Y. Wang, Y.C. Zhou, J. Wu, J. Heffernan, Oscillatory viral dynamics in a delayed HIV pathogenesis model, Math. Biosci. 219 (2009) 104–112.
[14] A. Sigal, J.T. Kim, et al., Cell-to-cell spread of HIV permits ongoing replication despite antiretroviral therapy, Nature 477 (2011) 95–98.
[15] A. Korobeinikov, Global properties of basic virus dynamics models, Bull. Math. Biol. 66 (2004) 879–883.
[16] M.Y. Li, J.S. Muldowney, A geometric approach to the global-stability problems, SIAM J. Math. Anal. 27 (1996) 1070–1083.
[17] R.T. Davey Jr., N. Bhat, C. Yoder, et al., HIV-1 and T cell dynamics after interruption of highly active antiretroviral therapy (HAART) in patients with a history of sustained viral suppression, Proc. Natl. Acad. Sci. USA 96 (1999) 15109–15114.
[18] T.-W. Chun, R.T. Davey Jr., D. Engel, et al., AIDS: re-emergence of HIV after stopping therapy, Nature 401 (1999) 874–875.
[19] T.-W. Chun, J.S. Justement, D. Murray, et al., Rebound of plasma viremia following cessation of antiretroviral therapy despite profoundly low levels of HIV reservoir: implications for eradication, AIDS 24 (2010) 2803–2808.
[20] E. Hamlyn, F.M. Ewings, K. Porter, et al., Plasma HIV viral rebound following protocol-indicated cessation of ART commenced in primary and chronic HIV infection, PLoS One 7 (2012) e43754.
[21] W. Huang, K.L. Cooke, C. Castillo-Chavez, Stability and bifurcation for a multiple-group model for the dynamics of HIV/AIDS transmission, SIAM J. Appl. Math. 52 (1992) 835–854.
[22] K.P. Hadeler, P. van den Driessche, Backward bifurcation in epidemic control, Math. Biosci. 146 (1997) 15–35.
[23] J. Dushoff, W. Huang, C. Castillo-Chavez, Backwards bifurcations and catastrophe in simple models of fatal diseases, J. Math. Biol. 36 (1998) 227–248.
[24] D. Greenhalgh, O. Diekmann, M.C.M. de Jong, Subcritical endemic steady states in mathematical models for animal infections with incomplete immunity, Math. Biosci. 165 (2000) 1–25.
[25] C.M. Kribs-Zaleta, M. Martcheva, Vaccination strategies and backward bifurcation in an age-since- infection structured model, Math. Biosci. 177–178 (2002) 317–332.
[26] P. van den Driessche, J. Watmough, Reproduction numbers and sub-threshold endemic equilibria for compartmental models of disease transmission, Math. Biosci. 180 (2002) 29–48.
[27] F. Brauer, Backward bifurcations in simple vaccination models, J. Math. Anal. Appl. 298 (2004) 418–431.
[28] J. Arino, K.L. Cooke, P. van den Driessche, J. Velasco-Hernández, An epidemiology model that includes a leaky vaccine with a general waning function, Discrete Contin. Dyn. Syst. Ser. B 4 (2004) 479–495.
[29] H. Gomez-Acevedo, M.Y. Li, Backward bifurcation in a model for HTLV-I infection of CD^{4+} T cells, Bull. Math. Biol. 67 (2005) 101–114.
[30] H. Wan, H. Zhu, The backward bifurcation in compartmental models for West Nile virus, Math. Biosci. 227 (2010) 20–28.
[31] K.W. Blayneh, A.B. Gumel, S. Lenhart, T. Clayton, Backward bifurcation and optimal control in transmission dynamics of West Nile virus, Bull. Math. Biol. 72 (2010) 1006–1028.
[32] M.Y. Li, J.R. Graef, L. Wang, J. Karsai, Global dynamics of a SEIR model with a varying total population size, Math. Biosci. 160 (1999) 191–213.
[33] H.I. Freedman, M.X. Tang, S.G. Ruan, Uniform persistence and flows near a closed positively invariant set, J. Dynam. Differential Equations 6 (1994) 583–600.
[34] G.J. Butler, P. Waltman, Persistence in dynamical systems, Proc. Amer. Math. Soc. 96 (1986) 425–430.
[35] R.H. Martin Jr., Logarithmic norms and projections applied to linear differential systems, J. Math. Anal. Appl. 45 (1974) 432–454.
[36] W.A. Coppel, Stability and Asymptotic Behavior of Differential Equations, Heath, Boston, 1995.
[37] J.V. Baker, G. Peng, J. Rapkin, et al., CD^{4+} count and risk of non-AIDS diseases following initial treatment for HIV infection, AIDS 22 (2008) 841–848.
[38] F. Antunes, Antiretroviral therapy for naive and for treatment-experienced HIV patients, and prevention of HIV transmission, Curr. Opin. HIV AIDS (Suppl. 1) (2011) S1–S2.
[39] D. Finzi, R. Siliciano, Viral dynamics in HIV-1 infection, Cell 93 (1998) 665–671.
[40] L. Rong, A.S. Perelson, Modeling HIV persistence, the latent reservoir, and viral blips, J. Theoret. Biol. 260 (2009) 308–331.
[41] J.M. Conway, D. Coombs, A stochastic model of latently infected cell reactivation and viral blip generation in treated HIV patients, PLoS Comput. Biol. 7 (2011) e1002033.
[42] M. Fiedler, Additive compound matrices and inequalities for eigenvalues of stochastic matrices, Czechoslovak Math. J. 99 (1974) 392–402.
[43] J.S. Muldowney, Compound matrices and ordinary differential equations, Rocky Mountain J. Math. 20 (1990) 857–872.